Variation in cell surface hydrophobicity among *Cryptococcus neoformans* strains influences interactions with amoeba

Raghav Vij[1¤], Conor J. Crawford[1,2], Arturo Casadevall[1]

[1]Department of Molecular Microbiology and Immunology, Johns Hopkins Bloomberg School of Public Health, Baltimore

[2]Centre for Synthesis and Chemical Biology, University College Dublin, Ireland

Running Head: Cell surface hydrophobicity of *C. neoformans* strains.

Corresponding author: Arturo Casadevall, acasade@jhu.edu

[¤]Current address: Department of Microbial Pathogenicity Mechanisms, Leibniz Institute for Natural Product Research and Infection Biology - Hans-Knöll-Institute, Jena, Germany

ABSTRACT

Cryptococcus neoformans and *Cryptococcus gattii* are pathogenic fungi that cause significant morbidity and mortality. Cell surface hydrophobicity (CSH) is a biophysical parameter that influences the adhesion of fungal cells or spores to biotic and abiotic surfaces. *C. neoformans* is encased by polysaccharide capsule that is highly hydrophilic and is a critical determinant of virulence. In this study, we report large differences in the CSH of some *C. neoformans* and *C. gattii* strains. The capsular polysaccharides of *C. neoformans* strains differ in repeating motifs, and therefore vary in the number of hydroxyl groups, which along with higher-order structure of the capsule, may contribute to the variation in hydrophobicity that we observed. For *C. neoformans*, CSH correlated with phagocytosis by natural soil predator *Acanthamoeba castellani*. Furthermore, capsular binding of the protective antibody (18B7), but not the non-protective (13F1) antibody altered the CSH of *C. neoformans* strains. Variability in CSH could be an important characteristic when comparing the biological properties of cryptococcal strains.

IMPORTANCE

The interaction of a microbial cell with its environment is influenced by the biophysical properties of a cell. The affinity of the cell surface for water, defined by the Cell Surface Hydrophobicity (CSH), is a biophysical parameter that varied amongst different strains of *Cryptococcus neoformans*. The CSH influenced the phagocytosis of the yeast by its natural predator in the soil, Amoeba. Studying variation in biophysical properties like CSH gives us insight into the dynamic host-predator interaction, and host-pathogen interaction in a damage-response framework.

KEYWORDS Cell surface hydrophobicity (CSH), *Cryptococcus neoformans*, *Cryptococcus gattii*, *Acanthamoeba castellanii*, capsular antibody, polysaccharide capsule

INTRODUCTION

The encapsulated basidiomycetes that comprise of the *Cryptococcus* species complex include several pathogenic species including *C. neoformans and C. gattii. Cryptococcus* spp. have a worldwide geographic distribution and are unusual among fungal pathogens, in that they have polysaccharide capsules that are essential for mammalian virulence.

Human infection usually begins in the lung. Infectious propagules of *C. neoformans*, in the form of spore or yeast, may be inhaled to cause a pulmonary infection that is usually cleared in immunocompetent hosts, or becomes latent. Conditions that impair immunity, such as HIV infection, are associated with disseminated disease, which usually manifests clinically as a meningoencephalitis. Recent evidence suggests that the nature of the infectious propagule has a significant effect on the outcome of the infection, as spores from *C. neoformans* cause significantly higher fungal burden in the brain of a murine model in comparison to small encapsulated yeast (1).

C. neoformans have been isolated from avian guano, soil, or arboreal sources. *C. gattii* has been isolated from trees, soil, freshwater, and seawater. There are three serotypes of *C. neoformans*, now referred to as *Cryptococcus neoformans* var. *neoformans* (Serotype D), *Cryptococcus neoformans* var. *grubii* (Serotype A) and hybrid (Serotype AD). Phylogenetic evidence suggests that they may be classified as separate species, *C. neoformans*, *C. deneoformans* and hybrid, respectively (2). Interestingly, *C.*

neoformans var. *grubii* has been isolated from 63% of clinical samples collected world-wide, followed by *C. neoformans* hybrid (6%), and *C. neoformans* var *neoformans* (5%) (3, 4). The genomic diversity in the Cryptococcal species complex may contribute to differences in the biophysical properties of cell surfaces within the *Cryptococcus* species complex.

C. neoformans and *C. gattii* cells are surrounded by a polysaccharide capsule that can dramatically vary in size during infection (5), and helps the pathogen evade the mammalian immune system. Highly branched polysaccharides (6) radiate outward form the cell wall, to form a dense matrix whose porosity increases with the distance from the cell wall (7). The capsule is primarily composed of glucuronoxylomannan (GXM, 98%), along with minor components galactoxylomannan and mannoproteins. GXM contains a core repeating structure of a α-(1→3)-mannose triad, with a β-(1→2) glucuronic acid branch on every third mannose (8). The capsule of different serotypes of *C. neoformans* and *C. gattii* have distinguishable polysaccharide motifs characterized by a varied degree of β-(1→2) or β-(1→4) xylose substitutions, and 6-*O*-acetyl substitutions along the mannan backbone (9). Polysaccharides are highly enriched in hydroxyl groups and form an extensive network of intramolecular and intermolecular hydrogen bonds, which includes bonding with water molecules. Therefore, polysaccharides are intrinsically hydrophilic molecules, which could provide an explanation for approximately 95% of the capsule's weight (10). Branching and substitution of polysaccharides effects the intra- and intermolecular hydrogen bonds and rigidity of the polymer, thereby effecting the polysaccharide's ability to form hydrogen bonds with water, which results variation in hydrophobicity (11–13).

Natural variation in biophysical parameters of the microbial surface of the *Cryptococcus* species complex has been previously described. Melanization, capsule induction, and binding of capsular antibody alter the cell surface charge, which also varies by strain (14). Chronological aging of the yeast and antibody binding alter the elasticity of the polysaccharide capsule that surrounds the *C. neoformans* cell (15, 16).

CSH is a property of a microbial surface that reflects the affinity of components of the microbe's cell surface for water and, is calculated by estimating the affinity of cell surfaces to hydrophobic substances like hydrophobic columns, solvents, or polystyrene beads (figure 1). The biological role of the CSH has been studied in bacteria such as *Staphylococcus aureus* and some fungi, and has succinctly reviewed in (17). Previous studies of *Candida albicans* have established the importance of CSH for the interaction of the pathogen with the host tissue (18). Furthermore, strain-specific variation in CSH of clinical isolates, and variation between species of *Candida* species complex have been reported (19).

The biophysical properties of the infectious propagule of *C. neoformans* in the form of yeast or spore influence the interaction of the yeast with its environment, and inside the host during infection. For example, during infection, *C. neoformans* interacts with lung epithelial cells, macrophages and can pass through the blood-brain barrier. In the environment, *Cryptococcus* species complex is believed to interact with amoeba (20) and, nematodes (21). Furthermore, hydrophobicity may influence the phagocytosis of microbial cells or particles by Amoeba (22).

In this study, we report variation in CSH of *C. neoformans* and *C. gattii* strains using two independent methods. Further, we observed that CSH correlated positively with

phagocytosis by *A. castellani*. Additionally, the higher order structure of the capsule is affected by the different capsular polysaccharide motifs, that vary between serotypes of *C. neoformans* and *C. gattii*, which may influence the CSH. We also found that binding of protective, but not non-protective antibodies altered the hydrophobicity of *C. neoformans* grown in capsule induction medium.

RESULTS

Cryptococcal spp. manifest significant differences in CSH.

Measuring CSH by the MATH and hydrophobic microsphere techniques (figure 1) revealed considerable variability among cells of *C. neoformans* and *C. gattii* strains cultured in Sabouraud Dextrose Broth (figure 2). By MATH assay, we found that serotype D strains B3501 and JEC21 were significantly more hydrophobic than the reference strain H99 (figure 2A). By the hydrophobic microsphere assay, we found that all strains of serotype D for which CSH was estimated, including B3501, ATCC24067 and JEC21, were significantly more hydrophobic than the reference strain H99 (figure 2B). However, there was considerable strain-to-strain variation and no pattern emerged regarding differences between serotypes or species, except for the notable finding that the most strains manifesting highest CSH were *C. neoformans* serotype D.

C. neoformans capsule and CSH.

The capsule is highly hydrophilic and is primarily composed of water (10). Hence, we sought to ascertain its contribution to CSH in *C. neoformans* strain H99 (serotype A) by comparing encapsulated H99, and non-encapsulated strain *CAP59*. To our surprise, we observed no major difference in CSH between H99 and *CAP59* cells grown in

Sabouraud-dextrose broth, by the MATH assay (p = 0.9988, figure 2A, table S1). However when grown in capsule inducing minimum medium (23), the non-encapsulated strain bound more hydrophobic beads than the encapsulated strains (figure 2B). Next, we compared the CSH of *C. neoformans* strain B3501 (serotype D) to the un-encapsulated strain *CAP67*, which has a mutation in *CAP59* gene of B3501 strain (24). We observed a significant decrease in the CSH by MATH assay (p = 0.0078, figure 2A, table S1).

Different strains and serotypes of *C. neoformans* and *C. gattii* have different dominant carbohydrate motifs in their capsule (9) that my influence the experimentally observed variation in CSH. To test this hypothesis, we used *in silico* method described by Mannhold *et. al* (25), to calculate and compare the lipophilicity (log *P*) of the four dominant GXM motifs. We observed the following trend in the predicted lipophilicity of GXM carbohydrate motifs; M4 (dominant in serotype C, log *P* 2.12) > M3 (dominant in serotype B, log *P* 2.01) > M2 (dominant in serotype A, log *P* 1.9) > M1 (dominant in serotype D, log *P* 1.79).

Based on the rationale that polysaccharides enriched in greater number of hydroxyl groups would have higher hydrophilicity, we counted the number of hydroxyl groups of each dominant GXM motif (figure 3). The M4 motif (dominant in serotype C) contained the highest number of hydroxyl groups, 21, followed by 19 hydroxyl groups in M3 (dominant in serotype B), 17 hydroxyl groups in M2 (dominant in serotype A) and 15 hydroxyl groups in M1 (dominant in serotype D).

CSH of unopsonized *C. neoformans* correlates with phagocytosis by *A. castellani*

148 To test whether CSH influences phagocytosis by soil predators like the amoeba, we
149 incubated fungal and protozoal cells and estimated the phagocytosis index. We found a
150 positive and linear correlation between CSH of *C. neoformans* strains and phagocytosis
151 index of *C. neoformans* strains by *A. castellanii* (figure 4).

152 **Effect of antibody binding on CSH**

153 Previous studies have demonstrated that capsule antibody binding alters capsule
154 structure and changes the surface charge of *C. neoformans* (14, 15). This led us to
155 investigate the effect of binding of capsular antibodies to *C. neoformans* on the CSH. We
156 demonstrated that binding of capsular antibody 18B7 (26) increases CSH in a
157 concentration-dependent manner, while binding of non-protective antibody 13F1 has no
158 significant effect on the CSH of *C. neoformans* cells grown in the capsule induction
159 medium (figure 5).

160

DISCUSSION

In this study, we measured the CSH of *C. neoformans* and found considerable inter-strain variation. When CSH was estimated by hydrophobic microsphere assay, *C. neoformans* serotype D strains were likely to be more hydrophobic than *C. neoformans* serotype A strain, with the caveat that we analyzed a relatively small set of strains from each serotype. We also demonstrated that CSH is a biophysical parameter that may influence the interaction of yeast cells with the environmental predator *Acanthamoeba castellani*. Finally, we demonstrated that the binding of a protective capsular antibody alters the CSH.

An earlier study suggested that capsule and protective anti-sera binding influenced hydrophobicity of *C. neoformans* (27). They reported no correlation between CSH and phagocytosis of *C. neoformans* by mouse peritoneal macrophages (27). The difference between our observations and the prior report may be attributed to the differences in methodologies. In the prior study, hydrophobicity was estimated from the number of cells that bound to hydrophobic columns. The cells were fixed with formalin, which may have altered surface properties of the yeast. In this study, we have used MATH assay that relies on the interaction of microbe with hydrophobic solvents to calculate CSH (figure 1A) (28). In addition, we have used hydrophobic microsphere assay that quantitates the interaction between hydrophobic beads and the yeast, visualized under a bright field microscope, to estimate the CSH (figure 1B) (18).

C. neoformans polysaccharide, like GXM, are essential components required in the formation of microbial communities called biofilms that are protective for the fungi (29). *C. neoformans* biofilms have been reported on medical devices (30, 31). Biofilm

associated cells have been associated with increased tolerance against antifungal drugs and phagocytic cells, as they upregulate proteins associated with host defense (32–34). In-vivo, *C. neoformans* form biofilm-like structures called cryptococcomas that could play a role in its neurotropism (35). The surface property of cells may affect the aggregation of microbial communities in biofilms. Interestingly, ATCC24067 and B3501 strains, that are highly hydrophobic also form biofilm more easily when compared to H99 strain that is relatively less hydrophobic (figure 1) (32, 33). A similar correlation between the formation of biofilm and CSH was observed a in *Candida* spp. (19, 36, 37) and in bacteria (38). Flocculation, another multicellular phenotype observed in yeasts, has been observed in *C. neoformans* cells during growth in certain medium (39), and could be caused by changes in CSH, as reported for brewer's yeast (40).

Amoebas are natural predators of *Cryptococcus* species (20, 41) and have emerged as a powerful tool for studying mechanism of intracellular pathogenesis and evolution of virulence (42, 43). A growing body of evidence suggests that virulence traits have emerged in environmental fungi, including *Cryptococcus* species, because of the selection pressure that results from fungi-amoeba interaction (44). Our finding that the more hydrophobic cryptococcal strains were more readily phagocytosed is congruent with the observation that Amoeba can phagocytose hydrophobic particles (22), although these mechanisms are not well understood. There is a remarkable correspondence between *C. neoformans* virulence traits that influence phagocytosis and enable survival of the fungi in *A. castellanii* and in human macrophages (42). For instance, the capsule of *C. neoformans* masks cell wall components that are recognized by innate immune receptors (45), and the absence of capsule leads to poor survival of *C. neoformans*

207 incubated with *A. castellanii* (42). In-vitro studies of macrophage and *C. neoformans*
208 interaction usually require opsonins such as capsular antibodies, and complement (46,
209 47) for phagocytosis by innate immune cells. As a result, what is known about the
210 immune response and phagocytosis of *C. neoformans* is greatly influenced by our
211 understanding of host cell receptor-opsonization agent interactions. Studying the effect
212 of CSH on phagocytosis in amoeba may give insights into factors independent of
213 opsonin-receptor interaction, which may influence phagocytosis in macrophages.

214 Murine antibodies that recognize capsular epitopes of *C. neoformans* can confer passive
215 protection to the host and enhance macrophage activity (48, 49). In addition to
216 facilitating phagocytosis of the yeast, the murine IgG antibody 18B7 (26) alters capsule
217 stiffness and impairs cellular replication of the yeast (15), significantly alters the cell
218 surface charge (14) and has a catalytic activity that breaks down the capsule (50). In this
219 study, we report that mAb 18B7 binding significantly increases the hydrophobicity of
220 *Cryptococcal* cell surface in a concentration-dependent manner, while non-protective
221 antibody, IgM 13F1, did not alter the CSH. We may attribute the differential effect of
222 changes in CSH induced by mAb 13F1 and 18B7 to the pattern of mAb binding, since
223 mAb18B7 binds near the surface in an annular pattern (15, 26, 51), while mAb 13F1
224 binds throughout the capsule in a punctate pattern (52, 53). There is precedence for our
225 observation in the encapsulated bacteria, *Klebsiella aerogenes*, where the pattern of
226 diffusion of some mAbs through the polysaccharide capsule has been shown to influence
227 the cell surface hydrophobicity (54, 55).

228 A surprising result in our study was that some *C. neoformans* strains manifest a
229 considerably higher CSH relative to others, despite being surrounded by a hydrophilic

capsule. The origin and mechanism for variability in CSH in these strains is not understood. Glycans are intrinsically hydrophilic molecules. Lipophilicity for glycans may be described by the partition coefficient (*P*), that is quantified as the distribution of a compound between two immiscible solvents, like water and octanol (56). While prior studies have compared the lipophilicity for monosaccharides, these efforts are not standardized in the field (13). For small molecules, log *P* can be accurately predicted by an equation proposed by Mannhold *et al.*, although the accuracy of the prediction decreases with an increase in non-hydrogen atoms (25). In this study we used this calculation to predict and compare the lipophilicity of capsular carbohydrate motifs (25), with the caveat that the suitability of these equations for molecules larger than monosaccharides is uncertain. The predicted calculated lipophilicity of GXM oligosaccharides motifs was positive, suggesting that the polymers would preferentially partition into an organic solvent. The M1 motif, which is dominant on the *C. neoformans* serotype D strains, was found to be less lipophilic in comparison to M3 and M4 motifs that are dominant in *C. gattii* serotype B and *C. neoformans* serotype A strains respectively (figure 3). This goes against our experimental observation that some *C. neoformans* serotype D strains were more hydrophobic than serotype B and A strains (figure 2) and implies that simple calculations of lipophilicity do not explain our findings. Instead, we suspect that discrepancy stems from higher-order polysaccharide structures that could present different molecular surfaces in their interaction with the solvent.

The dynamic nature of polysaccharides makes it challenging to obtain defined structures, and to relate the structure of glycans with their activity and biological roles.

Yet we know that the flexibility of the oligosaccharide polymer is influenced by intra- and intermolecular hydrogen bonds. Theoretical predictions suggest that α-(1→3)-mannan form weak intermolecular hydrogen bonds, resulting in a polymer with a flexible structure, that allows for many hydroxyl groups to interact with water (11). The primary component in the capsule of *C. neoformans*, is built upon repeating α-(1→3)-mannose triads, which would contribute to the observation that 95% of capsule's weight comes from water (10). We also found that the number of hydroxyl groups in each motif (figure 3), was inversely related to the observed CSH. The dominant motif M1 in the capsule of *C. neoformans* serotype D had fewer hydroxyl groups and the strains of serotype D tend to have higher CSH, when compared to the number hydroxyl group dominant motifs M2 and M3 of serotype A and B, whose strains had comparatively lower CSH. Fewer hydroxyl groups result in fewer opportunities for hydrogen bonding between the polysaccharide and water, which could translate into less hydrophilic structures with higher CSH.

It is also important to note that the motifs that enrich the capsule may differ between strains of the same serotype (9). For example, C. *neoformans* serotype D strain 24067 a capsular polysaccharide chemotyping suggests that M1 motif dominates 100% of the strain, while *C. neoformans* serotype D strain B3502 is composed of the dominant M1 (52%) motif, and M6 (48%) motif (9). This may contribute to the variation of CSH within strains grouped in serotype D (figure 2, Table S1).

Lipophilic structures have been reported in the capsule, which might extend to the surface and influence the hydrophobicity of the cell surface (11, 57). In addition, the composition of the cell wall, in particular the chitin-chitosan content in the cell wall,

that is regulated by CDA genes (58), may influence the hydrophobicity and adhesion of the yeast to various surface (59), a phenomenon that has also been reported in the plant pathogenic fungi *Magnoporthe orzaye* (60). The chemical structures responsible for the high CSH of some strains presents new puzzle for future study.

In summary, we report that CSH of *Cryptococcus* species can differ significantly depending on the strain. We have also demonstrated the correlation of the biophysical parameter CSH, with the phagocytosis by *A. castellanii* and that protective antibodies that bind to the capsule of *C. neoformans* may influence the hydrophobicity of *C. neoformans*. The finding that *C. neoformans* strain differ in CSH, and that changes to this cell-surface property correlates with biological properties, suggests the investigation of how this parameter is established and maintained could provide new insights into capsular structure.

289 # MATERIALS AND METHODS

290 ## Strains and culture of *C. neoformans* and *C. gattii*

291 *Cryptococcus neoformans* and *gattii* strains (Table 1) stored as frozen stocks at -80˚C
292 were streaked onto Sabouraud Agar plates and incubated at 30˚C for 48 hours. The
293 plates were stored at 4˚C for use up to 1 week. Multiple colonies were selected and
294 inoculated into 5 ml of liquid media, Sabouraud broth and incubated at 30˚C with
295 shaking. For capsule induction, 10^6 cells/ ml were washed 2X in PBS and inoculated into
296 MM (10 mM $MgSO_4$, 29.3 mM KH_2PO_4, 13 mM glycine, 3 µM thiamine-HCl, and
297 15 mM dextrose, with pH adjusted to 5.5).

298 ## Antibody incubation

299 *C. neoformans* (H99) grown in MM were washed 2X in PBS. Protective and non-
300 protective capsular antibodies, 18B7, 12A1, and 13F1 (61) respectively, were incubated
301 for 1 hour at 30˚C shaking. The CSH% was determined by MATH and microsphere
302 assays, as detailed below.

303 ## Estimation of CSH by MATH

304 CSH was estimated by MATH assay described in (28). Yeast cultures were washed 2X in
305 PBS and resuspended in 3 mL of PBS at an estimated Initial OD 0.2-0.4 recorded as A_0.
306 0.4 ml of n-Hexadecane was added, and the mixture was vortexed for 30 s and
307 incubated at 30˚C to allow the layers to separate. Final OD (A_1) of the aqueous layer was
308 recorded estimated as an average of 3 technical replicates in a 96 well plate read by
309 EMax Plus Microplate Reader (Molecular Devices). CSH% was estimated as $[1 -$
310 $(A_0/A_1)] \times 100$.

Estimation of CSH by hydrophobic microsphere assay

CSH of *C. neoformans* and *C. gattii* were estimated method detailed in (18) by resuspending 100 µL of 2 × 10^6 cells/ ml with 9.02 × 10^8 0.8 µm green hydrophobic beads (Bang Laboratories) in 2 mL of sodium phosphate buffer (0.05 M, pH 7.2) in clean glass tubes. After equilibration at RT for 2 minutes, the mixture was vortexed vigorously for 30 s. One hundred cells were counted, and the percentage of cells having >3 attached microspheres was considered as the CSH% value.

Acanthamoeba castellanii culture and phagocytosis index

Acanthamoeba castellanii strain 30234 was obtained from the American Type Culture Collection (ATCC). Cultures were maintained in PYG broth (ATCC medium 712) at 25°C according to instructions from ATCC.

Acanthamoeba castelanii phagocytosis index

The phagocytosis index was estimated as detailed in (62) with minor modifications. Briefly, 5 × 10^5 cells/ ml cells of *A. castellanii* were incubated in 35 mm No. 1.5 coverslip MatTek dishes with DPBS (Ca^{2+} and Mg^{2+}) for 3-4 hours. *C. neoformans* or *C. gattii* strains were incubated with 10 µg/mL Uvitex (fungal cell wall dye) and inoculated at MOI 1 and incubated for 2 hours at 25°C. The cells were imaged using Zeiss Axiovert 200M inverted microscope with 20× phase objective. Phagocytosis index was estimated by counting the number of *C. neoformans* or *C. gattii* engulfed per 100 amoeboid cells.

Estimation of lipophilicity and number of hydroxyl groups in carbohydrate motifs

Lipophilicity of the carbohydrate motif dominant in the capsule of *C. neoformans* serotype was estimated by method described by Mannhold *et al.* (25), as the log of the partition coefficient (*P*).

$$\log P = 1.46(\pm 0.02) + 0.11(\pm 0.001)\mathrm{NC} - 0.11(\pm 0.001)\mathrm{NHET}$$

Where NC is the number of carbon atoms in a molecule and NHET is the number of hetero atoms.

The number of hydroxyl groups in each motif of C. neoformans capsule was counted manually, as proxy for the number of hydrogen bond donor and acceptor atoms.

ACKNOWLEDGMENTS

A.C. was supported by grant 5R01HL059842. C.J.C. was funded by Irish Research Council postgraduate award (GOIPG/2016/998)

R.V. designed and conducted the experiments, analyzed the data, and wrote the manuscript. C.J.C. performed computation and theoretical analysis and wrote the manuscript. A.C. contributed to the experimental design, supervised the experiments, and edited and wrote parts of the manuscript. Special thanks to Radames JB Cordero for valuable discussions of experimental design and edits to the manuscript, and to Daniel Quinn Smith for the valuable contribution of editing the figures.

REFRENCES

1. Walsh NM, Botts MR, McDermott AJ, Ortiz SC, Wüthrich M, Klein B, Hull CM. 2019. Infectious particle identity determines dissemination and disease outcome for the inhaled human fungal pathogen Cryptococcus. PLOS Pathog 15:e1007777.

2. Kwon-Chung KJ, Bennett JE, Wickes BL, Meyer W, Cuomo CA, Wollenburg KR, Bicanic TA, Castañeda E, Chang YC, Chen J, Cogliati M, Dromer F, Ellis D, Filler SG, Fisher MC, Harrison TS, Holland SM, Kohno S, Kronstad JW, Lazera M, Levitz SM, Lionakis MS, May RC, Ngamskulrongroj P, Pappas PG, Perfect JR, Rickerts V, Sorrell TC, Walsh TJ, Williamson PR, Xu J, Zelazny AM, Casadevall A. 2017. The Case for Adopting the "Species Complex" Nomenclature for the Etiologic Agents of Cryptococcosis. mSphere 2:e00357-16.

3. Kwon-Chung KJ, Fraser JA, Doering TL, Wang Z, Janbon G, Idnurm A, Bahn Y-S. 2014. Cryptococcus neoformans and Cryptococcus gattii, the Etiologic Agents of Cryptococcosis. Cold Spring Harb Perspect Med 4.

4. Meyer W, Gilgado F, Ngamskulrungroj P, Trilles L, Hagen F, Castañeda E, Boekhout T. 2011. Molecular Typing of the Cryptococcus neoformans/Cryptococcus gattii Species Complex. Cryptococcus 327–357.

5. Charlier C, Chrétien F, Baudrimont M, Mordelet E, Lortholary O, Dromer F. 2005. Capsule Structure Changes Associated with Cryptococcus neoformans Crossing of the Blood-Brain Barrier. Am J Pathol 166:421–432.

6. Cordero RJB, Frases S, Guimaräes AJ, Rivera J, Casadevall A. 2011. Evidence for branching in cryptococcal capsular polysaccharides and consequences on its biological activity. Mol Microbiol 79:1101–1117.

7. Gates MA, Thorkildson P, Kozel TR. 2004. Molecular architecture of the Cryptococcus neoformans capsule. Mol Microbiol 52:13–24.

8. Cherniak R, Morris LC, Belay T, Spitzer ED, Casadevall A. 1995. Variation in the structure of glucuronoxylomannan in isolates from patients with recurrent cryptococcal meningitis. Infect Immun 63:1899–1905.

9. Cherniak R, Valafar H, Morris LC, Valafar F. 1998. Cryptococcus neoformans Chemotyping by Quantitative Analysis of 1H Nuclear Magnetic Resonance Spectra of Glucuronoxylomannans with a Computer-Simulated Artificial Neural Network. Clin Diagn Lab Immunol 5:146–159.

10. Maxson ME, Cook E, Casadevall A, Zaragoza O. 2007. The volume and hydration of the Cryptococcus neoformans polysaccharide capsule. Fungal Genet Biol FG B 44:180–186.

11. Almond A. 2005. Towards understanding the interaction between oligosaccharides and water molecules. Carbohydr Res 340:907–920.

12. Yu Y, Tyrikos□Ergas T, Zhu Y, Fittolani G, Bordoni V, Singhal A, Fair RJ, Grafmüller A, Seeberger PH, Delbianco M. 2019. Systematic Hydrogen-Bond Manipulations To Establish Polysaccharide Structure–Property Correlations. Angew Chem 131:13261–13266.

13. Fu DT, Oneill RA. 1995. Monosaccharide Composition Analysis of Oligosaccharides and Glycoproteins by High-Performance Liquid Chromatography. Anal Biochem 227:377–384.

14. Nosanchuk JD, Casadevall A. 1997. Cellular charge of Cryptococcus neoformans: contributions from the capsular polysaccharide, melanin, and monoclonal antibody binding. Infect Immun 65:1836–1841.

15. Cordero RJB, Pontes B, Frases S, Nakouzi AS, Nimrichter L, Rodrigues ML, Viana NB, Casadevall A. 2013. Antibody Binding to Cryptococcus neoformans Impairs Budding by Altering Capsular Mechanical Properties. J Immunol Author Choice 190:317–323.

16. Cordero RJB, Pontes B, Guimarães AJ, Martinez LR, Rivera J, Fries BC, Nimrichter L, Rodrigues ML, Viana NB, Casadevall A. 2011. Chronological Aging Is Associated with Biophysical and Chemical Changes in the Capsule of Cryptococcus neoformans. Infect Immun 79:4990–5000.

17. Krasowska A, Sigler K. 2014. How microorganisms use hydrophobicity and what does this mean for human needs? Front Cell Infect Microbiol 4.

18. Hazen KC, Brawner DL, Riesselman MH, Jutila MA, Cutler JE. 1991. Differential adherence of hydrophobic and hydrophilic Candida albicans yeast cells to mouse tissues. Infect Immun 59:907–912.

19. Borecká-Melkusová S, Bujdáková H. 2008. Variation of cell surface hydrophobicity and biofilm formation among genotypes of Candida albicans and Candida dubliniensis under antifungal treatment. Can J Microbiol 54:718–724.

20. Castellani A. 1930. An amoeba growing in cultures of a yeast. J Trop Med Hyg 33:188–191.

21. Mylonakis E, Ausubel FM, Perfect JR, Heitman J, Calderwood SB. 2002. Killing of Caenorhabditis elegans by Cryptococcus neoformans as a model of yeast pathogenesis. Proc Natl Acad Sci 99:15675–15680.

22. Vogel G, Thilo L, Schwarz H, Steinhart R. 1980. Mechanism of phagocytosis in dictyostelium discoideum: phagocytosis is mediated by different recognition sites as disclosed by mutants with altered phagocytotic properties. J Cell Biol 86:456–465.

415 23. Zaragoza O, Casadevall A. 2004. Experimental modulation of capsule size in Cryptococcus
416 neoformans. Biol Proced Online 6:10–15.

417 24. Vaishnav VV, Bacon BE, O'Neill M, Cherniak R. 1998. Structural characterization of the
418 galactoxylomannan of Cryptococcus neoformans Cap67. Carbohydr Res 306:315–330.

419 25. Mannhold R, Poda GI, Ostermann C, Tetko IV. 2009. Calculation of Molecular
420 Lipophilicity: State-of-the-Art and Comparison of LogP Methods on more than 96,000
421 Compounds. J Pharm Sci 98:861–893.

422 26. Casadevall A, Cleare W, Feldmesser M, Glatman-Freedman A, Goldman DL, Kozel TR,
423 Lendvai N, Mukherjee J, Pirofski LA, Rivera J, Rosas AL, Scharff MD, Valadon P, Westin
424 K, Zhong Z. 1998. Characterization of a murine monoclonal antibody to Cryptococcus
425 neoformans polysaccharide that is a candidate for human therapeutic studies. Antimicrob
426 Agents Chemother 42:1437–1446.

427 27. Kozel TR. 1983. Dissociation of a hydrophobic surface from phagocytosis of encapsulated
428 and non-encapsulated cryptococcus neoformans. Infect Immun 39:1214–1219.

429 28. Rosenberg M. 1984. Bacterial adherence to hydrocarbons: a useful technique for studying
430 cell surface hydrophobicity. FEMS Microbiol Lett 22:289–295.

431 29. Martinez LR, Casadevall A. 2007. Cryptococcus neoformans Biofilm Formation Depends
432 on Surface Support and Carbon Source and Reduces Fungal Cell Susceptibility to Heat,
433 Cold, and UV Light. Appl Environ Microbiol 73:4592–4601.

434 30. Banerjee U, Gupta K, Venugopal P. 1997. A case of prosthetic valve endocarditis caused by
435 Cryptococcus neoformans var. neoformans. J Med Vet Mycol Bi-Mon Publ Int Soc Hum
436 Anim Mycol 35:139–141.

437 31. Walsh TJ, Schlegel R, Moody MM, Costerton JW, Salcman M. 1986. Ventriculoatrial shunt
438 infection due to Cryptococcus neoformans: an ultrastructural and quantitative
439 microbiological study. Neurosurgery 18:373–375.

440 32. Martinez LR, Casadevall A. 2005. Specific antibody can prevent fungal biofilm formation
441 and this effect correlates with protective efficacy. Infect Immun 73:6350–6362.

442 33. Martinez LR, Casadevall A. 2006. Susceptibility of Cryptococcus neoformans biofilms to
443 antifungal agents in vitro. Antimicrob Agents Chemother 50:1021–1033.

444 34. Santi L, Beys-da-Silva WO, Berger M, Calzolari D, Guimarães JA, Moresco JJ, Yates JR.
445 2014. Proteomic profile of Cryptococcus neoformans biofilm reveals changes in metabolic
446 processes. J Proteome Res 13:1545–1559.

447 35. Aslanyan L, Sanchez DA, Valdebenito S, Eugenin EA, Ramos RL, Martinez LR. 2017. The
448 Crucial Role of Biofilms in Cryptococcus neoformans Survival within Macrophages and
449 Colonization of the Central Nervous System. J Fungi 3.

450 36. Bujdáková H, Didiášová M, Drahovská H, Černáková L. 2013. Role of cell surface
451 hydrophobicity in Candida albicans biofilm. Cent Eur J Biol 8:259–262.

452 37. Silva-Dias A, Miranda IM, Branco J, Monteiro-Soares M, Pina-Vaz C, Rodrigues AG. 2015.
453 Adhesion, biofilm formation, cell surface hydrophobicity, and antifungal planktonic
454 susceptibility: relationship among Candida spp. Front Microbiol 6.

455 38. Mirani ZA, Fatima A, Urooj S, Aziz M, Khan MN, Abbas T. 2018. Relationship of cell
456 surface hydrophobicity with biofilm formation and growth rate: A study on Pseudomonas
457 aeruginosa, Staphylococcus aureus, and Escherichia coli. Iran J Basic Med Sci 21:760–769.

458 39. Li L, Zaragoza O, Casadevall A, Fries BC. 2006. Characterization of a flocculation-like
459 phenotype in Cryptococcus neoformans and its effects on pathogenesis. Cell Microbiol
460 8:1730–1739.

461 40. Smit G, Straver MH, Lugtenberg BJ, Kijne JW. 1992. Flocculence of Saccharomyces
462 cerevisiae cells is induced by nutrient limitation, with cell surface hydrophobicity as a
463 major determinant. Appl Environ Microbiol 58:3709–3714.

464 41. Castellani A. 1955. [Phagocytic and destructive action of Hartmanella castellanii (Amoeba
465 castellanii) on pathogenic encapsulated yeast-like fungi Torulopsis neoformans
466 (Cryptococcus neoformans)]. Ann Inst Pasteur 89:1–7.

467 42. Steenbergen JN, Shuman HA, Casadevall A. 2001. Cryptococcus neoformans interactions
468 with amoebae suggest an explanation for its virulence and intracellular pathogenic strategy
469 in macrophages. Proc Natl Acad Sci 98:15245–15250.

470 43. Rizzo J, Albuquerque PC, Wolf JM, Nascimento R, Pereira MD, Nosanchuk JD, Rodrigues
471 ML. 2017. Analysis of multiple components involved in the interaction between
472 Cryptococcus neoformans and Acanthamoeba castellanii. Fungal Biol 121:602–614.

473 44. Casadevall A, Fu MS, Guimaraes AJ, Albuquerque P. 2019. The 'Amoeboid Predator-
474 Fungal Animal Virulence' Hypothesis. J Fungi 5:10.

475 45. O'Meara TR, Alspaugh JA. 2012. The Cryptococcus neoformans capsule: a sword and a
476 shield. Clin Microbiol Rev 25:387–408.

477 46. Kelly RM, Chen J, Yauch LE, Levitz SM. 2005. Opsonic Requirements for Dendritic Cell-
478 Mediated Responses to Cryptococcus neoformans. Infect Immun 73:592–598.

47. Zhong Z, Pirofski LA. 1996. Opsonization of Cryptococcus neoformans by human anticryptococcal glucuronoxylomannan antibodies. Infect Immun 64:3446–3450.

48. Mukherjee J, Scharff MD, Casadevall A. 1992. Protective murine monoclonal antibodies to Cryptococcus neoformans. Infect Immun 60:4534–4541.

49. Mukherjee S, Lee SC, Casadevall A. 1995. Antibodies to Cryptococcus neoformans glucuronoxylomannan enhance antifungal activity of murine macrophages. Infect Immun 63:573–579.

50. Bowen A, Wear MP, Cordero RJB, Oscarson S, Casadevall A. 2017. A Monoclonal Antibody to Cryptococcus neoformans Glucuronoxylomannan Manifests Hydrolytic Activity for Both Peptides and Polysaccharides. J Biol Chem 292:417–434.

51. Larsen RA, Pappas PG, Perfect J, Aberg JA, Casadevall A, Cloud GA, James R, Filler S, Dismukes WE. 2005. Phase I evaluation of the safety and pharmacokinetics of murine-derived anticryptococcal antibody 18B7 in subjects with treated cryptococcal meningitis. Antimicrob Agents Chemother 49:952–958.

52. Feldmesser M, Rivera J, Kress Y, Kozel TR, Casadevall A. 2000. Antibody Interactions with the Capsule ofCryptococcus neoformans. Infect Immun 68:3642–3650.

53. MacGill TC, MacGill RS, Casadevall A, Kozel TR. 2000. Biological Correlates of Capsular (Quellung) Reactions of Cryptococcus neoformans. J Immunol 164:4835–4842.

54. Held TK, Jendrike NRM, Rukavina T, Podschun R, Trautmann M. 2000. Binding to and Opsonophagocytic Activity of O-Antigen-Specific Monoclonal Antibodies against Encapsulated and NonencapsulatedKlebsiella pneumoniae Serotype O1 Strains. Infect Immun 68:2402–2409.

501 55. Williams P, Lambert PA, Brown MRW. 1988. Penetration of immunoglobulins through the
502 Klebsiella capsule and their effect on cell-surface hydrophobicity. J Med Microbiol 26:29–
503 35.

504 56. Chiou CT, Freed VH, Schmedding DW, Kohnert RL. 1977. Partition coefficient and
505 bioaccumulation of selected organic chemicals. Environ Sci Technol 11:475–478.

506 57. Nicola AM, Frases S, Casadevall A. 2009. Lipophilic dye staining of Cryptococcus
507 neoformans extracellular vesicles and capsule. Eukaryot Cell 8:1373–1380.

508 58. Upadhya R, Baker LG, Lam WC, Specht CA, Donlin MJ, Lodge JK. 2018. Cryptococcus
509 neoformans Cda1 and Its Chitin Deacetylase Activity Are Required for Fungal
510 Pathogenesis. mBio 9.

511 59. Teixeira PAC, Penha LL, Mendonça-Previato L, Previato JO. 2014. Mannoprotein MP84
512 mediates the adhesion of Cryptococcus neoformans to epithelial lung cells. Front Cell
513 Infect Microbiol 4.

514 60. Geoghegan IA, Gurr SJ. 2016. Chitosan Mediates Germling Adhesion in Magnaporthe
515 oryzae and Is Required for Surface Sensing and Germling Morphogenesis. PLOS Pathog
516 12:e1005703.

517 61. Mukherjee J, Casadevall A, Scharff MD. 1993. Molecular characterization of the humoral
518 responses to Cryptococcus neoformans infection and glucuronoxylomannan-tetanus toxoid
519 conjugate immunization. J Exp Med 177:1105–1116.

520 62. Fu MS, Casadevall A. 2018. Divalent Metal Cations Potentiate the Predatory Capacity of
521 Amoeba for Cryptococcus neoformans. Appl Environ Microbiol 84:e01717-17.

63. Steenbergen JN, Casadevall A. 2000. Prevalence of Cryptococcus neoformans var. neoformans (Serotype D) and Cryptococcus neoformans var. grubii (Serotype A) Isolates in New York City. J Clin Microbiol 38:1974–1976.

64. Cleare W, Casadevall A. 1998. The Different Binding Patterns of Two Immunoglobulin M Monoclonal Antibodies to Cryptococcus neoformans Serotype A and D Strains Correlate with Serotype Classification and Differences in Functional Assays. Clin Diagn Lab Immunol 5:125–129.

65. Heitman J, Allen B, Alspaugh JA, Kwon-Chung KJ. 1999. On the Origins of Congenic MATα and MATa Strains of the Pathogenic Yeast Cryptococcus neoformans. Fungal Genet Biol 28:1–5.

66. Freij JB, Fu MS, De Leon Rodriguez CM, Dziedzic A, Jedlicka AE, Dragotakes Q, Rossi DCP, Jung EH, Coelho C, Casadevall A. 2018. Conservation of Intracellular Pathogenic Strategy among Distantly Related Cryptococcal Species. Infect Immun 86.

67. Varki A, Cummings RD, Aebi M, Packer NH, Seeberger PH, Esko JD, Stanley P, Hart G, Darvill A, Kinoshita T, Prestegard JJ, Schnaar RL, Freeze HH, Marth JD, Bertozzi CR, Etzler ME, Frank M, Vliegenthart JF, Lütteke T, Perez S, Bolton E, Rudd P, Paulson J, Kanehisa M, Toukach P, Aoki-Kinoshita KF, Dell A, Narimatsu H, York W, Taniguchi N, Kornfeld S. 2015. Symbol Nomenclature for Graphical Representations of Glycans. Glycobiology 25:1323–1324.

543 **TABLES**

544 **Table 1:** Strains of *C. neoformans* and *C. gattii* used in the present study. The
545 references indicate the study in which the strains were serotyped, or the study in which
546 the strains used had been characterized by serotype.

Species		Mutant	Serotype	Source
Cryptococcus neoformans	H99		A	John Perfect (Durham, NC)
		CAP59		
	J45			(63)
	J10			(63)
	J43			(63)
	J48			(63)
	SB6			(64)
	MAS92-203		AD	(6)
	ATCC24067		D	(6)
	B3501			(6)
		CAP67		
	JEC21			(65)
	J39			(63)
Cryptococcus gattii	R265		B	ATCC (Manassas, VA) (66)
	NIH444			(6)
	WM179			ATCC (Manassas, VA)(66)

547

548

549 **FIGURES**

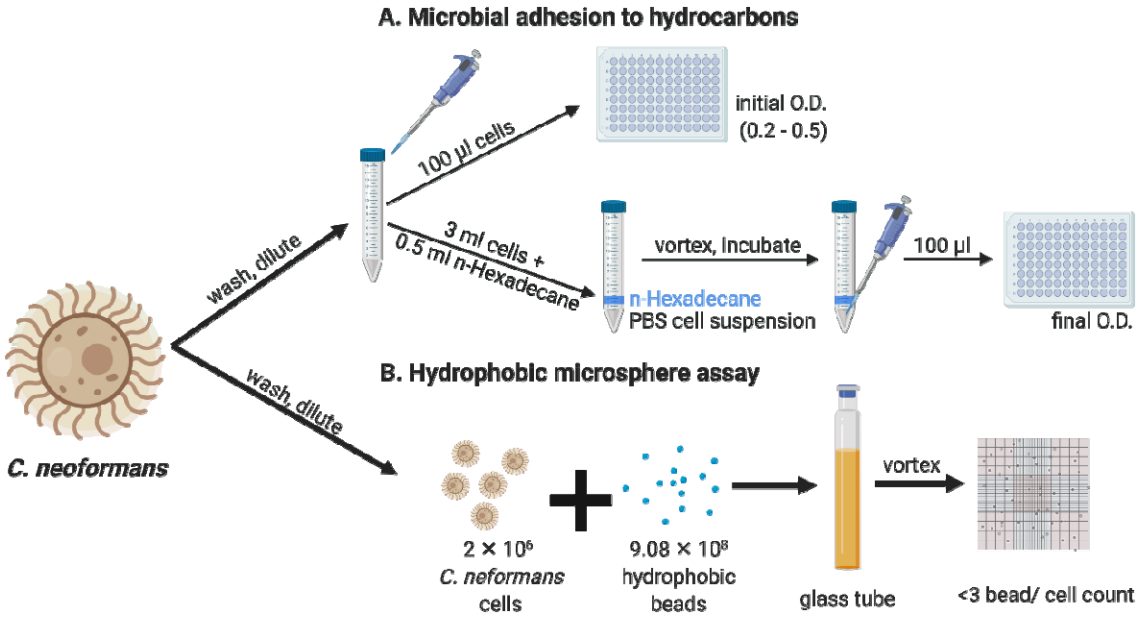

550

551 **Figure 1: Methods for estimation of *C. neoformans* CSH. A.** CSH estimated by
552 MATH assay that quantifies the interaction of *C. neoformans* cells in a suspension with the
553 hydrocarbon solvent n-Hexadecane. CSH% was calculated as the percentage change in OD of a
554 *C. neoformans* cell suspension after vortexing the mixture of cells with n-Hexadecane. **B.** In
555 addition, we estimated CSH by visualizing the interaction between *C. neoformans* cells and
556 hydrophobic beads (0.8 µm) in a hemocytometer and counting cells that had >3 beads/ 100 cells
557 to calculate CSH%. Image created with BioRender.

558

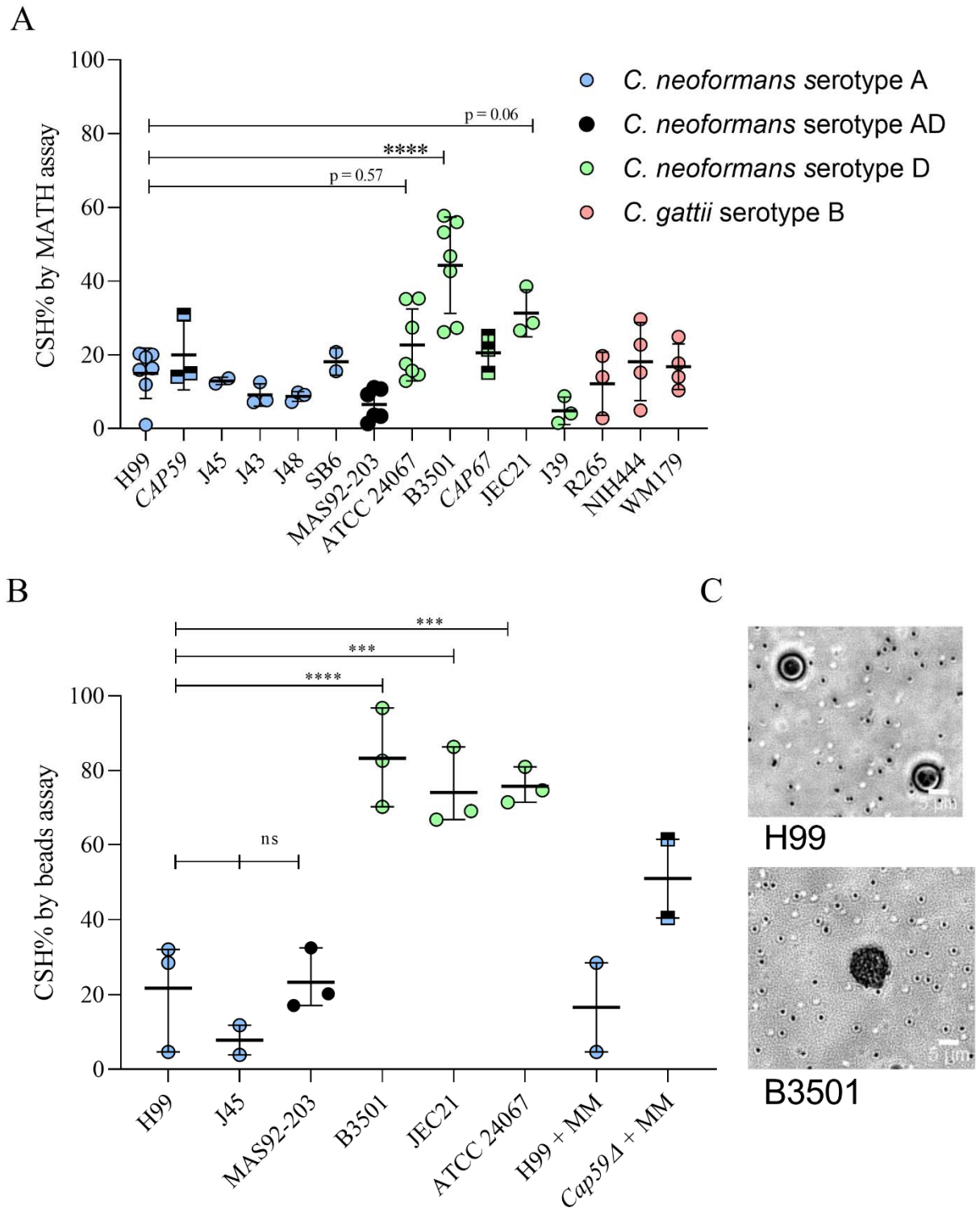

559
560 **Figure 2: CSH of *C. neoformans* differs by strain.** Graphical representation of

561 CSH of *C. neoformans* and *C. gattii* strains. **A.** Graphical representation of CSH
562 estimated by MATH assay. **B.** Graphical representation of CSH estimated by
563 hydrophobic microsphere assay (left). Experiments have been performed 2-6 times
564 independently, as indicated by individual data points. (○) Indicates a data point of CSH
565 of an encapsulated strain of *C. neoformans* and *C. gattii*, while, (□) indicates the CSH of
566 an acapsular mutant of the preceding *C. neoformans* strain (starting from the y-axis).
567 Error bar represents the standard deviation about of mean. **C.** Representative image of a
568 mixture hydrophobic beads with *C. neoformans* strain H99 (upper right) and relatively
569 hydrophobic *C. neoformans* strain B3501 (lower right) used for the assay. Hydrophobic
570 beads (small spheres, approximately 0.8μm in diameter) adhere to the cell surface due
571 to the high hydrophobicity of B3501 cell, covering it almost completely. The
572 hydrophobic beads are all but absent from the surface of H99 cells. Ordinary one-way
573 ANOVA was used to compare the CSH of *C. neoformans* strain H99 with the CSH of *C.*
574 *neoformans* and *C. gattii* strains (supplementary materials table S2). The following
575 symbols were used to annotate the statistical significance of the results: ns, $p > 0.05$;
576 *, $p \leq 0.05$; **, $p \leq 0.01$; ***, $p \leq 0.001$; ****, $p \leq 0.0001$.

577

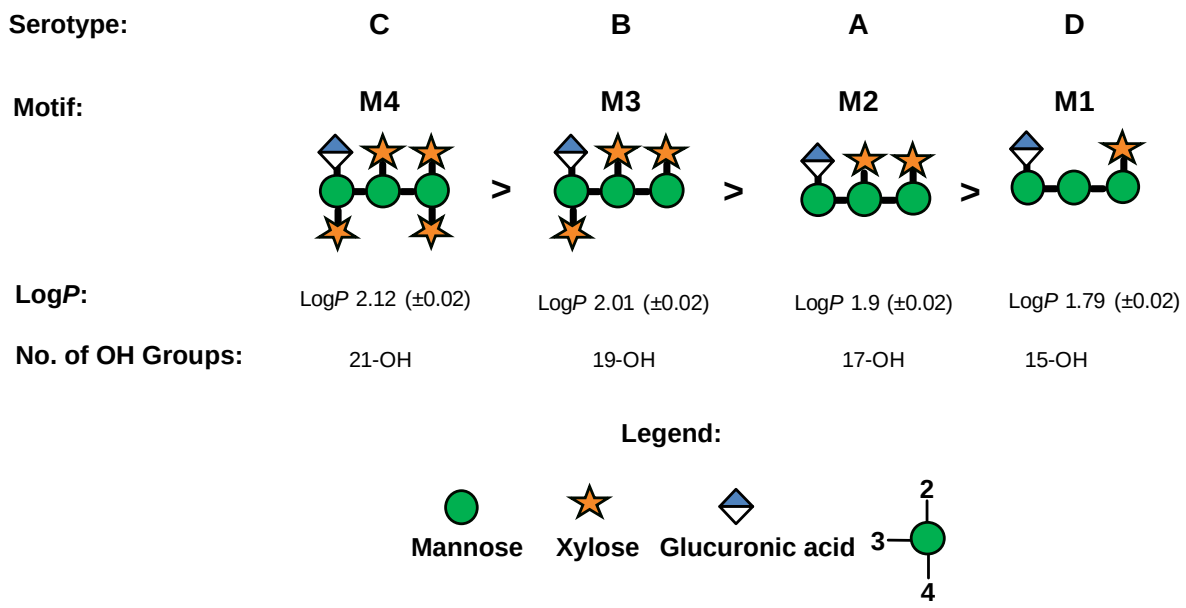

Figure 3: Comparison of hydrophobicity between different capsule motifs dominant in *C. neoformans* and *C. gattii*. Lipophilicity, log *P*, of dominant carbohydrate motifs in the carbohydrate was predicted by an equation proposed by Mannhold *et. al* (25). M4 was found to be the most hydrophobic motif and M1 the least. The number of hydroxyl groups on each polysaccharide motif was calculated (below). Glycan notification followed the Symbol Nomenclature for Glycans (SNFG) (67).

587

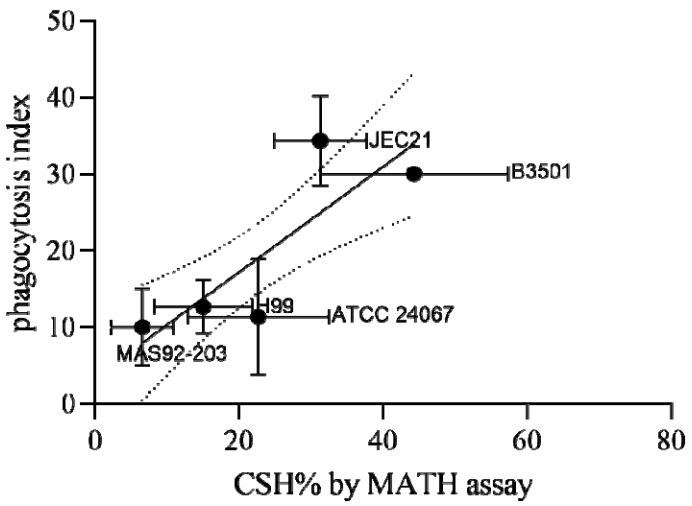

588

589 **Figure 4: CSH of *C. neoformans* correlates with phagocytosis of *C.***
590 ***neoformans* by natural predator *A. castellani*.** Significant positive linear
591 correlation (R^2 = 0.5722) between CSH of C. *neoformans* strains and phagocytosis index
592 by *A. castellanii*. Phagocytosis index is estimated by fluorescence microscopy as the
593 number of *C. neoformans* labeled by Uvitex internalized per 100 *A. castellanii*. Error
594 bar represents the standard deviation of the mean.

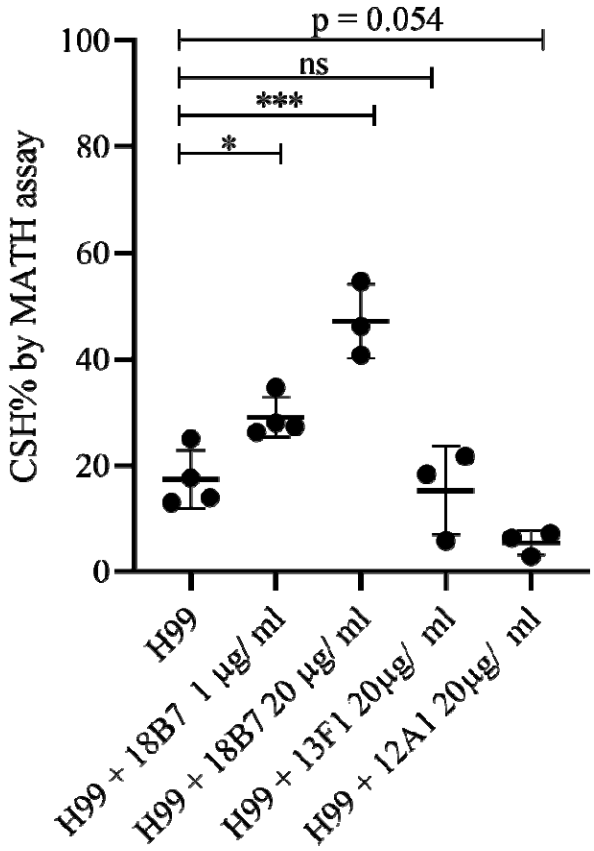

Figure 5: Binding of protective capsule antibodies influences CSH. Incubation of *C. neoformans* strain H99 grown in the capsule induction medium (MM) with protective capsular antibodies 18B7 significantly increase CSH in a concentration-dependent manner, while 12A1 decreased CSH and 13F1 had no significant effect on CSH. CSH was determined by MATH assay in 2-3 biological replicates, as indicated by data points. Error bar represents the standard deviation about the mean. Ordinary one-way ANOVA was used to compare the CSH of untreated *C. neoformans* strain H99 with the CSH of H99 cells treated with different antibodies. The following symbols were used to annotate the statistical significance of the results: ns, p>□0.05; *, p□≤□0.05; **, p□≤□0.01; ***, p□≤□0.001; ****, p□≤□0.0001.

606 **SUPPLEMENTARY MATERIAL**

607 **Supplementary Table S1:** Table summarizing the results of multiple comparison of
608 CSH% by MATH assay by ordinary one-way ANOVA, where mean of each column was
609 compared to the mean of the other, (graphical representation in figure 2A).

Tukey's multiple comparisons test	Mean Diff.	95.00% CI of diff.	Significant?	Summary	Adjusted P Value
B3501 vs. H99	29.28	13.80 to 44.76	Yes	****	<0.0001
B3501 vs. ATCC 24067	21.62	6.141 to 37.10	Yes	***	0.0008
B3501 vs. MAS92-203	37.74	21.62 to 53.85	Yes	****	<0.0001
B3501 vs. R265	32.13	12.14 to 52.11	Yes	****	<0.0001
B3501 vs. WM179	27.53	9.382 to 45.69	Yes	***	0.0002
B3501 vs. NIH444	26.13	7.975 to 44.28	Yes	***	0.0005
B3501 vs. J43	35.15	15.17 to 55.13	Yes	****	<0.0001
B3501 vs. SB6	26.12	2.905 to 49.34	Yes	*	0.0149
B3501 vs. JEC21	13.01	-6.970 to 33.00	No	ns	0.5717
B3501 vs. J45	31.36	8.136 to 54.57	Yes	**	0.0013
B3501 vs. J48	35.57	15.58 to 55.55	Yes	****	<0.0001
B3501 vs. J39	39.49	19.51 to 59.47	Yes	****	<0.0001
B3501 vs. *CAP59*	24.32	4.335 to 44.30	Yes	**	0.0057
B3501 vs. *CAP67*	23.73	3.743 to 43.71	Yes	**	0.0078
H99 vs. ATCC 24067	-7.659	-23.14 to 7.820	No	ns	0.896
H99 vs. MAS92-203	8.456	-7.656 to 24.57	No	ns	0.8496
H99 vs. R265	2.846	-17.14 to 22.83	No	ns	>0.9999
H99 vs. WM179	-1.747	-19.90 to 16.40	No	ns	>0.9999
H99 vs. NIH444	-3.154	-21.31 to 15.00	No	ns	>0.9999
H99 vs. J43	5.87	-14.11 to 25.85	No	ns	0.999

H99 vs. SB6	-3.156	-26.38 to 20.06	No	ns	>0.9999
H99 vs. JEC21	-16.27	-36.25 to 3.718	No	ns	0.227
H99 vs. J45	2.075	-21.14 to 25.29	No	ns	>0.9999
H99 vs. J48	6.285	-13.70 to 26.27	No	ns	0.9979
H99 vs. J39	10.21	-9.774 to 30.19	No	ns	0.8723
H99 vs. *CAP59*	-4.961	-24.95 to 15.02	No	ns	0.9998
H99 vs. *CAP67*	-5.553	-25.54 to 14.43	No	ns	0.9994
ATCC 24067 vs. MAS92-203	16.11	0.003366 to 32.23	Yes	*	0.0499
ATCC 24067 vs. R265	10.51	-9.479 to 30.49	No	ns	0.8481
ATCC 24067 vs. WM179	5.913	-12.24 to 24.06	No	ns	0.9969
ATCC 24067 vs. NIH444	4.505	-13.65 to 22.66	No	ns	0.9998
ATCC 24067 vs. J43	13.53	-6.455 to 33.51	No	ns	0.509
ATCC 24067 vs. SB6	4.503	-18.72 to 27.72	No	ns	>0.9999
ATCC 24067 vs. JEC21	-8.607	-28.59 to 11.38	No	ns	0.9619
ATCC 24067 vs. J45	9.734	-13.48 to 32.95	No	ns	0.9693
ATCC 24067 vs. J48	13.94	-6.040 to 33.93	No	ns	0.4594
ATCC 24067 vs. J39	17.87	-2.114 to 37.85	No	ns	0.1243
ATCC 24067 vs. *CAP59*	2.698	-17.29 to 22.68	No	ns	>0.9999
ATCC 24067 vs. *CAP67*	2.106	-17.88 to 22.09	No	ns	>0.9999
MAS92-203 vs. R265	-5.61	-26.09 to 14.87	No	ns	0.9995
MAS92-203 vs. WM179	-10.2	-28.90 to 8.491	No	ns	0.8115
MAS92-203 vs. NIH444	-11.61	-30.30 to 7.084	No	ns	0.6453
MAS92-203 vs. J43	-2.586	-23.06 to 17.89	No	ns	>0.9999
MAS92-203 vs. SB6	-11.61	-35.26 to 12.03	No	ns	0.9011
MAS92-203 vs. JEC21	-24.72	-45.20 to -4.244	Yes	**	0.0063
MAS92-203 vs. J45	-6.381	-30.03 to 17.26	No	ns	0.9996

MAS92-203 vs. J48	-2.171	-22.65 to 18.31	No	ns	>0.9999
MAS92-203 vs. J39	1.755	-18.72 to 22.23	No	ns	>0.9999
MAS92-203 vs. *CAP59*	-13.42	-33.89 to 7.061	No	ns	0.5621
MAS92-203 vs. *CAP67*	-14.01	-34.49 to 6.469	No	ns	0.4919
R265 vs. WM179	-4.592	-26.71 to 17.53	No	ns	>0.9999
R265 vs. NIH444	-6	-28.12 to 16.12	No	ns	0.9996
R265 vs. J43	3.024	-20.62 to 26.67	No	ns	>0.9999
R265 vs. SB6	-6.002	-32.44 to 20.43	No	ns	>0.9999
R265 vs. JEC21	-19.11	-42.76 to 4.534	No	ns	0.2361
R265 vs. J45	-0.7708	-27.21 to 25.67	No	ns	>0.9999
R265 vs. J48	3.439	-20.21 to 27.08	No	ns	>0.9999
R265 vs. J39	7.365	-16.28 to 31.01	No	ns	0.9981
R265 vs. *CAP59*	-7.807	-31.45 to 15.84	No	ns	0.9965
R265 vs. *CAP67*	-8.399	-32.04 to 15.25	No	ns	0.9929
WM179 vs. NIH444	-1.407	-21.88 to 19.07	No	ns	>0.9999
WM179 vs. J43	7.616	-14.50 to 29.73	No	ns	0.9947
WM179 vs. SB6	-1.41	-26.49 to 23.67	No	ns	>0.9999
WM179 vs. JEC21	-14.52	-36.64 to 7.599	No	ns	0.559
WM179 vs. J45	3.822	-21.26 to 28.90	No	ns	>0.9999
WM179 vs. J48	8.031	-14.09 to 30.15	No	ns	0.9912
WM179 vs. J39	11.96	-10.16 to 34.08	No	ns	0.8213
WM179 vs. *CAP59*	-3.214	-25.33 to 18.90	No	ns	>0.9999
WM179 vs. *CAP67*	-3.806	-25.92 to 18.31	No	ns	>0.9999
NIH444 vs. J43	9.024	-13.09 to 31.14	No	ns	0.9755
NIH444 vs. SB6	-0.00231	-25.08 to 25.08	No	ns	>0.9999
NIH444 vs. JEC21	-13.11	-35.23 to 9.006	No	ns	0.7118

NIH444 vs. J45	5.229	-19.85 to 30.31	No	ns	>0.9999
NIH444 vs. J48	9.439	-12.68 to 31.56	No	ns	0.9646
NIH444 vs. J39	13.36	-8.754 to 35.48	No	ns	0.6853
NIH444 vs. *CAP59*	-1.807	-23.93 to 20.31	No	ns	>0.9999
NIH444 vs. *CAP67*	-2.399	-24.52 to 19.72	No	ns	>0.9999
J43 vs. SB6	-9.026	-35.46 to 17.41	No	ns	0.9951
J43 vs. JEC21	-22.14	-45.78 to 1.510	No	ns	0.0879
J43 vs. J45	-3.795	-30.23 to 22.64	No	ns	>0.9999
J43 vs. J48	0.4152	-23.23 to 24.06	No	ns	>0.9999
J43 vs. J39	4.341	-19.30 to 27.99	No	ns	>0.9999
J43 vs. *CAP59*	-10.83	-34.48 to 12.81	No	ns	0.9392
J43 vs. *CAP67*	-11.42	-35.07 to 12.22	No	ns	0.9114
SB6 vs. JEC21	-13.11	-39.55 to 13.33	No	ns	0.8945
SB6 vs. J45	5.231	-23.73 to 34.19	No	ns	>0.9999
SB6 vs. J48	9.441	-17.00 to 35.88	No	ns	0.9925
SB6 vs. J39	13.37	-13.07 to 39.80	No	ns	0.8805
SB6 vs. *CAP59*	-1.805	-28.24 to 24.63	No	ns	>0.9999
SB6 vs. *CAP67*	-2.397	-28.83 to 24.04	No	ns	>0.9999
JEC21 vs. J45	18.34	-8.095 to 44.78	No	ns	0.4688
JEC21 vs. J48	22.55	-1.094 to 46.20	No	ns	0.0756
JEC21 vs. J39	26.48	2.831 to 50.12	Yes	*	0.0157
JEC21 vs. *CAP59*	11.31	-12.34 to 34.95	No	ns	0.9175
JEC21 vs. *CAP67*	10.71	-12.93 to 34.36	No	ns	0.9439
J45 vs. J48	4.21	-22.23 to 30.65	No	ns	>0.9999
J45 vs. J39	8.136	-18.30 to 34.57	No	ns	0.9983
J45 vs. *CAP59*	-7.036	-33.47 to 19.40	No	ns	0.9996
J45 vs. *CAP67*	-7.628	-34.06 to 18.81	No	ns	0.9991

J48 vs. J39	3.926	-19.72 to 27.57	No	ns	>0.9999
J48 vs. *CAP59*	-11.25	-34.89 to 12.40	No	ns	0.9204
J48 vs. *CAP67*	-11.84	-35.48 to 11.81	No	ns	0.8878
J39 vs. *CAP59*	-15.17	-38.82 to 8.474	No	ns	0.5953
J39 vs. *CAP67*	-15.76	-39.41 to 7.882	No	ns	0.534
CAP59 vs. *CAP67*	-0.5919	-24.24 to 23.05	No	ns	>0.9999

610

611

Supplementary Table S2: Table summarizing the results of multiple comparison of mean CSH% by MATH assay by ordinary one-way ANOVA, where mean of each column was compared to the mean of *C. neoformans* strain H99 (graphically representation in figure 2A).

Dunnett's multiple comparisons test	Mean Diff.	95.00% CI of diff.	Significant?	Summary	Adjusted P Value
H99 vs. B3501	-29.28	-42.24 to -16.32	Yes	****	<0.0001
H99 vs. ATCC 24067	-7.659	-20.62 to 5.298	No	ns	0.5766
H99 vs. MAS92-203	8.456	-5.031 to 21.94	No	ns	0.4971
H99 vs. R265	2.846	-13.88 to 19.57	No	ns	0.9994
H99 vs. WM179	-1.747	-16.94 to 13.45	No	ns	0.9996
H99 vs. NIH444	-3.154	-18.35 to 12.04	No	ns	0.9992
H99 vs. J43	5.87	-10.86 to 22.60	No	ns	0.9738
H99 vs. SB6	-3.156	-22.59 to 16.28	No	ns	0.9994
H99 vs. JEC21	-16.27	-32.99 to 0.4622	No	ns	0.0615
H99 vs. J45	2.075	-17.36 to 21.51	No	ns	0.9996
H99 vs. J48	6.285	-10.44 to 23.01	No	ns	0.9567
H99 vs. J39	10.21	-6.518 to 26.94	No	ns	0.5337
H99 vs. *CAP59*	-4.961	-21.69 to 11.77	No	ns	0.9908
H99 vs. *CAP67*	-5.553	-22.28 to 11.18	No	ns	0.9837